Journal of Technology and Value Addition
Vol. 8, Issue No. 2, July 2026, pp. 50-67
https://www.uwu.ac.lk/jtva/
ISSN: 3051-5203 (Online)

Research Article

Molecular-level exploration of Curcumin rotamers; conformational effects on HDAC8 recognition, drug-likeness and pharmacological potential.

O.A.D.B. Perera and G. Parthiban*

Department of Chemistry, Faculty of Science, Eastern University Sri Lanka, Chenkalady 30350, Sri Lanka

*Correspondence: parthibang@esn.ac.lk; Tel.: +94 77 233 4187

Abstract

Curcumin, a bioactive compound obtained from the rhizome of *Curcuma longa*, has been widely investigated for its potential anti-cancer properties. It has also been reported to interact with Histone Deacetylases (HDACs) which are involved in the regulation of gene expression. However, its therapeutic potential is hindered by poor solubility, chemical instability and restricted bioavailability. With the focus of overcoming these limitations, this study was arranged to identify Curcumin and its isomers as potential anti-cancer agents. However, comparative computational investigations of Curcumin isomers, including diketo and enol forms in Dimethyl Sulfoxide (DMSO) media remain limited. This study employed a multifaced computational approach involving DFT-based geometry optimization and frequency calculations using B3LYP/6-31+G(d) method, followed by pKa prediction in DMSO, molecular docking, QSAR analysis and in-silico ADMET and toxicity evaluation using pkCSM and SwissADME. Molecular docking results indicated that the studied Curcumin rotamers exhibited weak to moderate HDAC8 binding affinities based on predicted binding free energies and estimated Ki values. QSAR analysis provided predicted pIC_{50} values from molecular descriptors, which were evaluated separately from the docking-derived binding energies and estimated Ki values. These computationally derived parameters were interpreted as distinct measures of binding affinity and predicted inhibitory potency, while the ADMET and drug-likeness analyses indicated generally favourable predicted pharmacokinetic and toxicity related profiles for the studied rotamers. Overall, the findings provide preliminary computational insights into the HDAC8 binding characteristics, molecular descriptors and predicted pharmacokinetic profiles of Curcumin isomers. However, experimental validation is required to confirm these predictions and establish their biological and anticancer relevance.

Keywords: Adsorption Distribution Metabolism Excretion and Toxicity (ADMET), Curcumin, Density Functional Theory (DFT), Histone Deacetylase Enzyme (HDAC), Quantitative Structure Activity Relationship (QSAR)

This article is published under the Creative Commons Attribution License (https://creativecommons.org/licenses/by/4.0/), which permits unrestricted use, distribution, and reproduction in any medium, provided the original work is properly cited.

1. Introduction

Curcumin [1,7-bis (4-hydroxy-3 methoxyphenyl)-1,6-heptadiene-3,5-dione] (Naama *et al.*, 2013) is considered a valuable therapeutic agent due to its exceptional antioxidant and anti-inflammatory properties (Nag *et al.*, 2018). Ayurvedic medicine Curcumin is used to treat chronic diseases and cancers (Truong *et al.*, 2025). In modern medical advancements Curcumin is recognized as a natural inhibitor of the HDAC enzyme, which causes the suppression of tumor (Li and Seto, 2016; Ferrari, 2024). However, the valuable therapeutic potential of Curcumin is limited by its poor bioavailability, chemical instability, and low solubility (Mahal *et al.*, 2024). Previous computational studies related to DFT theory, molecular docking and ADMET analysis have investigated the pharmacokinetic and molecular properties of Curcumin (Mahal *et al.*, 2024). However, those computational studies have given limited attention to the combined effects of conformational variability, solvent environment, and pharmacokinetic properties when evaluating different Curcumin isomers. In particular, a systematic comparative computational investigation of the diketo and enol forms of Curcumin in DMSO, integrating structural, electronic, binding, QSAR, and ADMET perspectives remains limited.

Investigation of both rotameric and diketo forms is important because rational changes can alter the three-dimensional conformation of Curcumin while keto-enol tautomerism can modify its electronic structure and hydrogen-bonding characteristics, potentially affecting predicted target interactions. Therefore, this study addresses the central research question of how conformational and tautomeric variations influence the molecular, electronic, HDAC8 binding and pharmacokinetic properties of Curcumin in DMSO. It was hypothesized these structural variations would produce measurable differences in calculated molecular properties and predicted HDAC8 interactions. Accordingly, the present study aimed to comparatively investigate selected Curcumin rotamers and the diketo form in DMSO using an integrated computational framework. Specifically, the objectives were to characterize their structural and electronic properties using DFT calculations, predict pKa values in DMSO, assess predicted HDAC8 binding interactions through molecular docking, examine structure-activity relationships using QSAR analysis and evaluate predicted pharmacokinetic properties through in-silico ADMET analysis. These objectives were addressed through a sequential computational workflow in which DFT calculations were first used to characterize the optimized structures and electronic properties followed by pka prediction, molecular docking against HDAC8, QSAR analysis, and in-silico ADMET and toxicity evaluation (Nag *et al.*, 2018). This method can be considered an efficient alternative to experimental techniques since it is cost-effective and reduces the usage of valuable chemicals (Mahal *et al.*, 2024). Therefore, this integrated approach was designed to provide a more comprehensive computational understanding of the structure-property-activity relationships of Curcumin isomers and to identify promising candidates for further experimental investigation. As a preliminary, hypothesis-generating study, further experimental

validation and docking protocol refinement are required to confirm the predicted HDAC8 inhibitory potential and establish the anticancer relevance of the Curcumin isomers.

2. Materials and Methods

2.1. Identification of Enol Rotamer Structures and Diketone Form

Curcumin's different rotamers were identified by considering the four different rotation axes including two (C-C) single bonds and the two (C-Ph) single bonds. For easy understanding the letters "a" and "b" were added to illustrate the two possible orientations of OCH_3 around C-Ph bond. S-cis and s-trans were indicated by considering the conformational orientations of $C^{11} – H^{36}$ bond regard to the C^{12}-O^{26} and of C^{15}-H^{38} bond about C^{14}-O^{27} respectively (Kolev *et al.*, 2005).

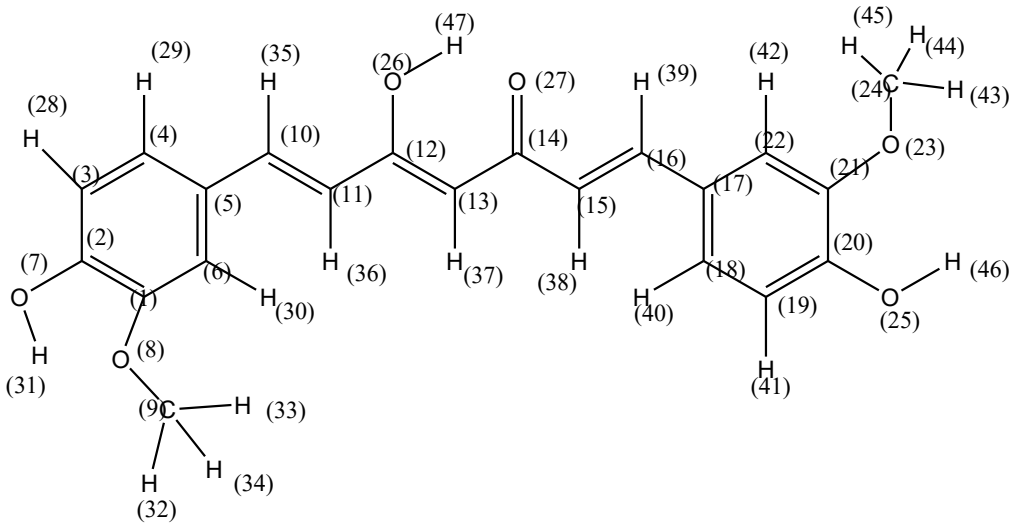


Figure 1. Numbering the atoms of 2D Curcumin scaffold.

2.2. Geometry Optimization and Frequency Calculation

Ten different conformational molecular structures were analyzed using Gaussian 09 software package. Full geometry optimizations and frequency calculations (opt+freq) were carried out separately for each Curcumin rotamer in the neutral gas phase, neutral solvent phase, deprotonated structures in gas phase and deprotonated structures in solvent phase. The conformational isomers of Curcumin were investigated using DFT method with the B3LYP hybrid functional, which incorporates approximate electron-correlation effects using the 6-31+G(d) basis set. Structures exhibiting no imaginary frequencies were considered local minima and treated as energetically favourable conformations representing plausible tautomeric states. To improve the numerical accuracy an ultrafine integration grid was employed. DMSO was used as ligand preparation solvent (Solvation Model based on Density) (Boulmokh *et al.*, 2024).

2.3 pka Calculation for Each Isomer in DMSO Media

The pKa values of the selected Curcumin isomers in DMSO were estimated using a thermodynamic cycle combining gas-phase deprotonation and solvation free energies. Gibbs free energies for the neutral (HA) and deprotonated (A^-) forms were obtained from the converged DFT frequency calculations, considering deprotonation at the phenolic site. The gas phase proton free energy, ($\Delta G_{(gas)}H^+ = -6.28\ kcal\ mol^{-1}$) and proton solvation free energy were combined to obtain the solution phase Gibbs free energies, including the appropriate 1 atm to 1M standard state correction of 1.90 kcal mol^{-1} where required (Mckee and Pogorelov, 2019; Alisi *et al.*, 2020; ALI *et al.*, 2021). Here, HA denotes the Curcumin in neutral state and A^- denotes the Curcumin anion after removal of H^+ ion from the phenolic site (Nedyalkova *et al.*, 2019).

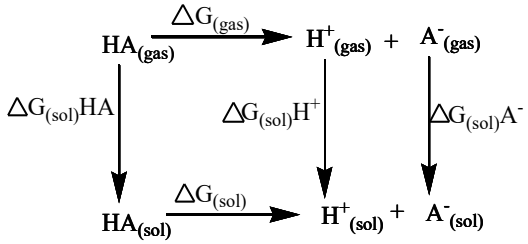


Figure 2. Diagrammatic representation of the thermodynamic cycle designed by ChemDraw tool.

$$\Delta G_{(sol)}HA = G_{(sol)}HA - G_{(gas)}HA \quad (1)$$

$$\Delta G_{(sol)}A^- = G_{(sol)}A^- - G_{(gas)}A^- \quad (2)$$

$\Delta G_{(sol)}H^+ = -270\ kcal\ mol^{-1}$ (ALI *et al.*, 2021) (3)

$\Delta G_{(gas)}H^+ = -6.28\ kcal\ mol^{-1}$ (ALI *et al.*, 2021) (4)

$$\Delta G_{(gas)} = \left[G_{(gas)}H^+ + G_{(gas)}A^-\right] - G_{(gas)}HA \quad (5)$$

Usual correction value =1.90 kcal mol^{-1} (ALI *et al.*, 2021)

Accordingly,

$$\Delta G_{(sol)} = [-\Delta G_{(sol)}HA] + \Delta G_{(gas)} + \Delta G_{(sol)}H^+ + \Delta G_{(sol)}A^- \quad (6)$$

Then pka was calculated as below equation,

$pka = \Delta G_{(sol)}/2.303RT$ (Ali *et al.*, 2021) (7)

$$2.303\ RT = 1.364\ kcal\ mol^{-1} \quad (8)$$

2.4. Implementing Docking Studies for the Curcumin Rotamers and HDAC Enzyme

HDAC8 (PDB ID:1ZZ1) was selected as molecular target because its dysregulation has been associated with cancer progression and HDAC8 inhibition has been investigated as a potential strategy for anticancer drug development. Biovia Discovery Studio, developed by Dassault Systems was used for preparation of required files. Water molecules, extraneous small molecules, cofactors and ligands were removed from the imported protein by using the "Hierarchy viewer". Rotamer structures in the DMSO media were considered as the ligands for the target 1ZZ1 protein structure. Energy minimized converged Gaussian output files were converted into the (.pdbqt) format by using the OpenBabel software. Once the enzyme and the ligands were properly prepared, molecular docking was implemented by using AutoDock Tools 1.5.7 and the AutoDock4 engine. The docking grid was defined with 40*40*40 points, a spacing of 0.375 Å and a grid center of (-3.969, 5.352, 15.593) Å. The Lamarckian Genetic Algorithm (LGA) was employed with 10 independent runs, a population size of 150, 2500000 maximum energy evaluations, 27000 maximum generations, an elitism value of 1, mutation rate of 0.8. AutoDock4 distance dependent dielectric treatment was used with a dielectric parameter of -0.1465 and smoothing parameter of 0.5 Å, incorporating atom-specific affinity, electrostatic, and desolvation maps for scoring. Docking poses were ranked primarily according to predicted binding free energy, with estimated Ki values and ligand-HDAC8 interactions considered for pose interpretation. Docking was performed separately for each Curcumin rotamer to enable comparative assessment of predicted HDAC-binding characteristics. In addition, docking scores were analyzed on a per-conformation basis without assuming a single averaged binding energy, due to the interconvertible nature of Curcumin tautomers. Range-based reporting was used to reflect variability across conformations. As redocking-based validation was not performed, the docking results were considered comparative computational predictions rather than experimentally validated binding affinities. The specific interactions between best pose and protein were visualized by using the Discovery Studio software. For further analysis or imaging, the best pose was saved in the (.pdb) format.

2.5. Theoretical IC_{50} Estimation

AutoDock 4 is an important computational tool for predicting the free energy of ligand binding to the active site. Further it gives information about Inhibition constant (K_i). K_i is the theoretical estimate of how tightly ligand binds to the active site (Spassov, 2024). The conversion of docking-derived binding free energies to estimated Ki assumed a thermodynamic relationship. Using below equation Ki was calculated.

$$\Delta G\ Binding\ Energy = RT\ lnK_i \quad (9)$$

$$IC_{50} = e^{\frac{\Delta G}{RT}} \quad (10)$$

The estimated Ki values were subsequently related to IC_{50} using Cheng-Prusoff Equation;

$$Ki = \frac{IC50}{1 + \frac{[S]}{K_m}} \quad (11)$$

When $[S] << K_m$, $IC_{50} \approx K_i$ means that in low-substrate assays.

Here [S] is the substrate concentration and K_m is the Michaelis Constant. Because the required experimental [S] and K_m values were not determined in the present computational study, the resulting values were treated as estimated rather than experimental IC_{50} values.

2.6. QSAR Analysis (Multiple Regression Analysis and Prediction of Drug likeness)

A Multiple Linear Regression (MLR) analysis was performed using Microsoft Excel to investigate the relationship between selected molecular descriptors and the calculated pIC_{50} values. The molecular descriptors were used as independent variables, while pIC_{50} was used as the dependent variable. Statistical significance was assessed at $p < 0.05$, and the coefficient of determination (R^2), adjusted R^2, standard error and p values of the regression coefficients were used to evaluate the preliminary model.

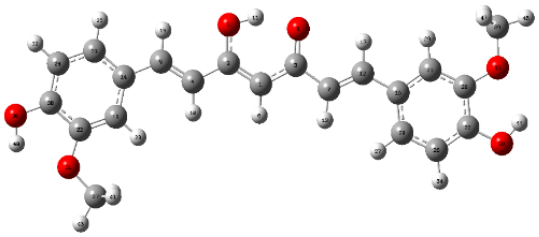
A separate QSAR analysis was performed by using ChemMaster Software to demonstrate drug-likeness value. The dataset of Chemical structures was converted into .sdf format by using OpenBabel software and loaded into the ChemMaster software. A number of descriptors including physicochemical properties, structural features, electronic properties and 2D/3D descriptors were calculated for each structure. The data set was split into a training set and a test set by using random or clustering methods and the selected descriptors were used to develop the multiple linear regression model

2.7. In Silico Toxicology Analysis (Prediction of ADMET properties)

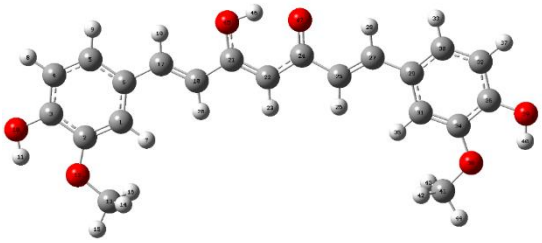
The SMILES structures of each rotamer were generated from the OpenBabel software by converting from the optimized neutral solvent phase of the Gaussian output files. Next separate SMILES formats were pasted into SwissADME and all the structures were run as a batch. After completion of running process, important sections like physicochemical, pharmacokinetics, BOILED-EGG, Medicinal chemistry, Solubility and Bioavailability scores were checked for analysis. But a separate SMILES format was accepted by the pkCSM online tool one at a time to interpret the results. After the completion of running, ADMET properties were checked under physiological assumptions for the evaluation of drug candidates.

3. Results and Discussion

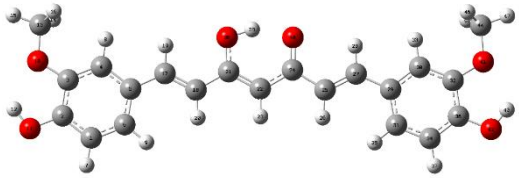
3.1. Structure Identification



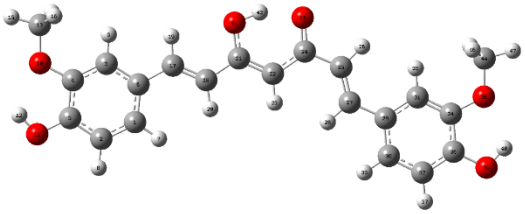
(a)



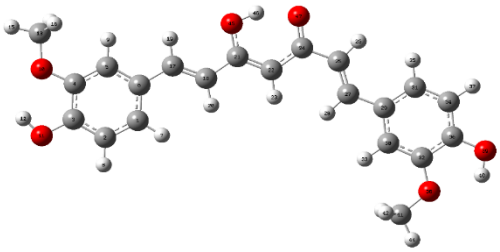
(b)



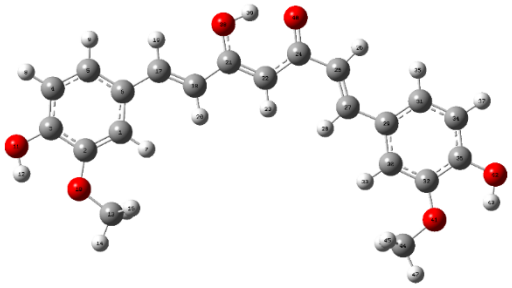
(c)



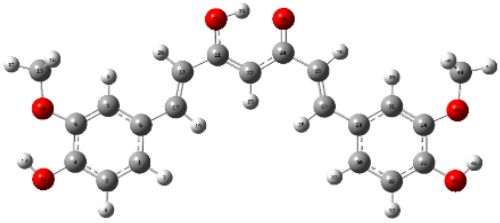
(d)



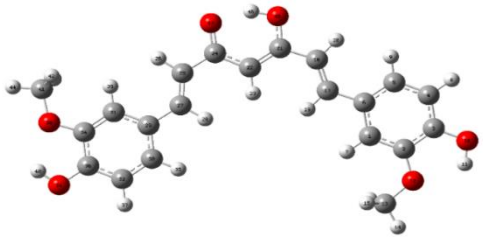
(e)



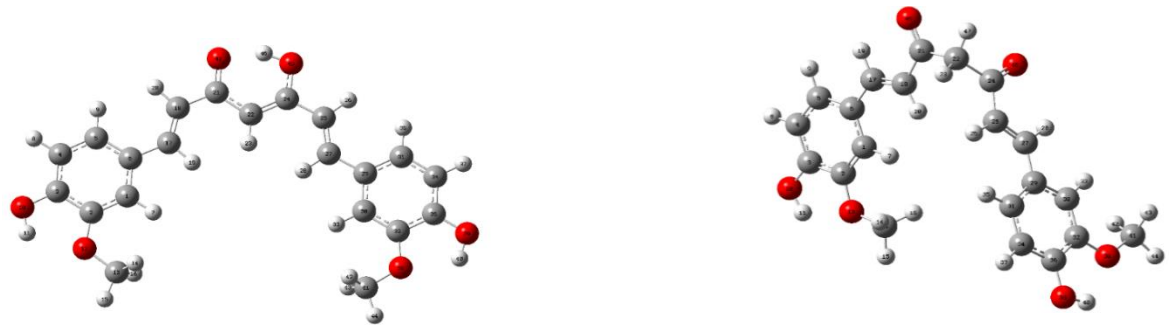
(f)



(g)



(h)



(i) (j)

Figure 3. Optimized structures of the neutral Curcumin with DFT method 6-31G+ (d) basis set and B3LYP functional; (a) a, s-trans, s-trans, b (b) a, s-trans, s-trans, a (c) b, s-trans, s-trans, b (d) b, s-trans, s-cis, b (e) a, s-trans, s-cis, b (f) a, s-trans, s-cis, a (g) b, s-cis, s-cis, b (h) a, s-cis, s-cis, b (i) a, s-cis, s-cis, a (j) Diketone.

3.2. Pka Calculation

Table 1. Calculated pka values for Curcumin rotamers.

Compound	Calculated pka value
a	-15.07
b	-16.93
c	-15.60
d	-16.05
e	-15.10
f	-15.47
g	-15.35
h	-15.26
i	-15.22
j	-15.47

The computed pKa values for Curcumin rotamers were negative, ranging from -15.10 to -16.93. These highly negative absolute values reflect an exceptionally strong predicted propensity for deprotonation under calculated conditions, the remarkably narrow variation among them provides critical insight into the molecule's electronic structure. The relatively small variation in pKa among the rotamers suggests that conformational changes have only a minor effect on the calculated acid-base properties (Boulmokh *et al.*, 2024). A s-trans, s-trans, a conformer resulted in the lowest calculated pKa value (-16.93), indicating the greatest predicted tendency toward deprotonation among the investigated conformers. Mechanistically, this suggests that the extended π conjugation framework of Curcumin backbone acts as the primary thermodynamic driver of acidity. Furthermore, the diketone tautomer exhibited a similar pKa value, indicating that tautomerism does not significantly alter the acidity profile in DMSO. Ultimately, these findings shift the focus of Curcumin's reactivity away from the conformational dynamics, establishing that its fundamental acid-base behaviour is almost entirely governed by its macro-electronic conjugation.

3.3 Molecular Docking Scores of Curcumin rotamers using AutoDock4.

Table 2. Binding energies, Inhibitory constants and IC_{50} values of Curcumin isomers using AutoDock4.

Compound	Binding Energy (kcal mol^{-1})	Inhibitory Constant, Ki (µM)	IC_{50} Value (µM)
a	-4.67	376.32	376.32
b	-4.76	324.10	324.10
c	-5.11	178.12	178.12
d	-4.59	429.16	429.16
e	-4.55	462.51	462.51
f	-4.45	547.19	547.19
g	-4.67	375.85	375.85
h	-4.71	352.47	352.47
i	-4.19	850.23	850.23
j	-3.56	2450.00	2450.00

Docking binding energies (ΔG) were transformed into estimated inhibition constants (Ki) using thermodynamic relationships. The corresponding Ki values were used as surrogate metric for relative binding strength. For internal ranking purpose, these values were treated as docking-derived inhibitory descriptors, rather than experimentally determined Ki or IC_{50} values and should be interpreted only as approximate comparative indicators of predicted binding strength. More negative predicted binding energies correspond to lower estimated Ki values and, under the stated assumptions, lower estimated IC_{50} values. The more negative predicted binding energies indicate relatively stronger predicted interactions with the HDAC8 binding site. The predicted binding poses suggest that Curcumin tautomers interact with residues within the HDAC8 catalytic binding region, including regions associated with the Zn^{+2} containing active site and hydrophobic channel.

According to the above data, the ΔG values ranged from (-3.56 to -5.11 kcal mol^{-1}), with more negative values representing relatively stronger predicted interactions. Among the obtained Gibbs free energy values the b, s-trans, s-trans, b structure was considered to have the lowest energy and K_i values in the dataset, which contributed to the strongest interactions. The diketone structure possessed the largest binding energy and K_i value, indicating that its binding was poorer than that of all the other enol structures. The s-trans structures tend to be more stable and better bound than the s-cis structures. This may indicate that changes in conformation, such as tautomeric shifts, can significantly affect the docking affinity (Spassov, 2024). The main enol forms are stabilized through hydrogen bonding which forms stronger binding (Nag *et al.*, 2018). The s-trans compounds allow for better alignment of π electrons which makes favorable interactions with protein residues. Since these structures have optimal geometries for interacting with the active site of the target.

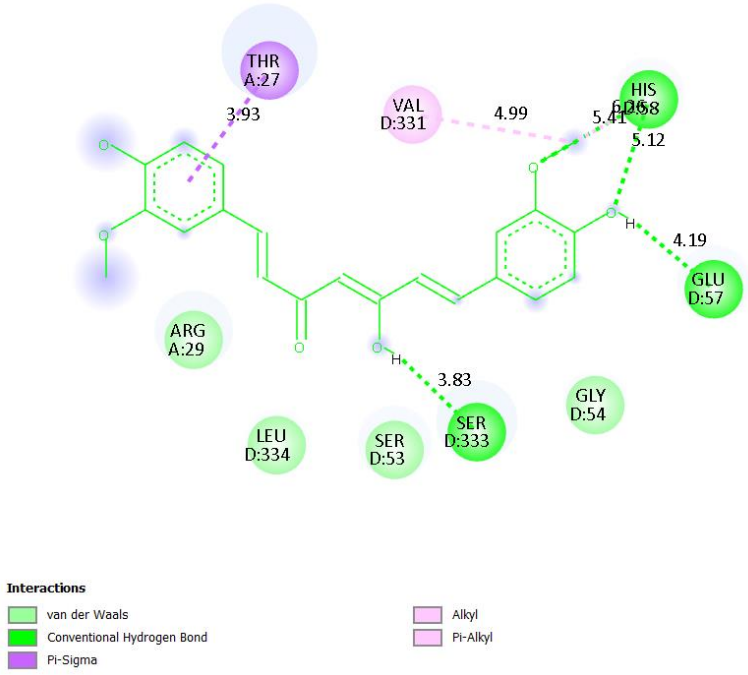


Figure 4. 2D binding interaction diagram of a, s-trans, s-trans, b and 1ZZ1 By using Discovery Studio.

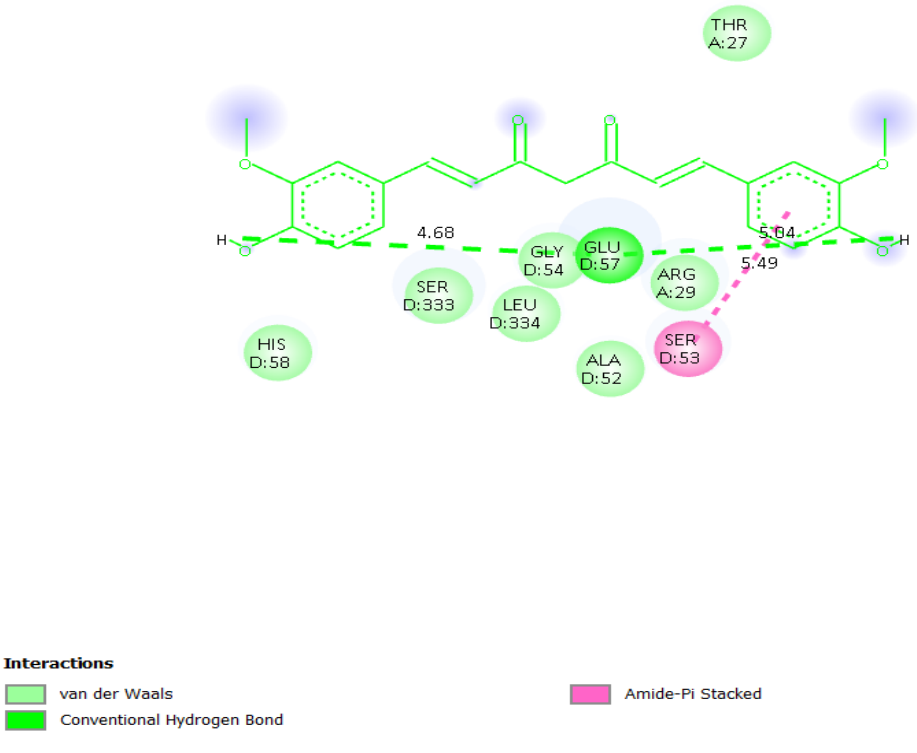


Figure 5. 2D binding interaction diagram of Diketone and 1ZZ1 by using Discovery Studio

3.4. QSAR Analysis of Rotamers

3.4.1. Multiple Regression Analysis in Excel

Preliminary QSAR analysis (R^2 = 0.80, Adjusted R^2 = 0.71, Standard Error = 0.16) demonstrated that HOMO energy (p = 0.01) significantly correlated with pIC_{50} values ranging from 2.61 to 3.75 (3.32 ± 0.30) whereas the dipole moment (p = 0.11) and pKa (p = 0.28) showed weaker and non-significant contributions. Chemically, this indicates that higher HOMO energy donates electrons more readily (Bonab *et al.*, 2017). Within the HDAC active site, this electronic profile likely facilitates superior coordination with the catalytic Zn^{2+} ion or enhances charge-transfer interactions with electrophilic amino acid residues. (Boulmokh *et al.*, 2024).

The dipole moment was not statistically significant in this mode. Although it appears in the model, its contribution to pIC_{50} was weak; this means that polarity among the isomers does not strongly affect their inhibitory activity. The negative coefficient indicated that a lower pKa (more acidic derivatives) slightly increases the activity, but the effect is small and not reliable enough to be considered predictive. These results demonstrate that HDAC inhibition by curcumin is an orbital-controlled process, where the ease of localized electron donation outweighs macro-environmental electrostatic or acidic behaviour.

The resulting QSAR model can be expressed as,

$$pIC_{50} = (-0.02411251) \times Dipole\ Moment + 76.63945256 \times HOMO\ Energy$$

$$+ (-0.116510466) \times pka + 16.60524224$$

This equation provides a preliminary quantitative description of the relationship between the three descriptors and the calculated pIC_{50} values. However, overfitting remains a concern because of the limited data set and the absence of independent validation. Therefore, the model should be considered exploratory rather than a validated predictive model.

3.4.2. QSAR Analysis in drug likeness prediction by using ChemMaster

The Quantitative Structure Activity Relationship parameters of the rotameric and tautomeric forms of curcumin were analyzed to determine the influence of conformational variation on molecular properties and drug likeness. According to the above results, enolic form displayed identical molecular characteristics with molecular weight of 368.385 g mol^{-1}, log P = 3.8526 and molar refractivity = 103.104. These values imply that conformational rotations around Carbon and Carbon Single bonds do not significantly alter the hydrophobicity or polarizability of the molecule. Each enolic form has six Hydrogen bond acceptors, three hydrogen bond donors and twelve rotatable bonds, allowing for the high conformational flexibility. Since Curcumin can adopt its geometry during protein-ligand interactions and form multiple Hydrogen bonding and Vander Waals interactions within biological targets. The estimated drug likeness values

for all enolic forms (0.3902) suggested moderate compliance with Lipinski's rule of five, indicating a favourable balance between solubility and permeability.

In contrast, transitioning from the enol to diketone tautomer triggers a profound shift in both lipophilicity and predicted bioavailability. The reduction in log P from 3.8526 (enol) to 3.3699 (diketone) can be attributed to the disruption of the strong intramolecular hydrogen-bonding network. Inherent to the enol's planar heptadienone core. While the enol form masks its polar Oxygen atoms within this intramolecular hydrogen-bonding network. Thereby artificially inflating its lipophilicity and the diketone form eliminates this structural constraint. This exposes carbonyl groups to the microenvironment, lowering log P, reducing molar refractivity and directly driving the drug-likeness index upward from 0.3902 to 0.5481.

Although both enolic and diketone forms fulfill the general requirements for drug-like behaviour, the diketone form possesses the superior predicted bioavailability. This enhanced ability of the diketone form will contribute for efficient absorption, distribution and membrane transport which are essential parameters in biological activity and pharmacodynamics. Therefore, while the highly conjugated enol rotamers may remain essential for localized electronic interactions and chelation within the HDAC active site, the diketone tautomer likely acts as the primary vehicle responsible for efficient systemic delivery and cellular permeation.

Table 1. QSAR analysis for the Curcumin rotamers with different parameters.

Comp.	Molecular Weight	Log P	Molar Refractivity	H bond Acceptors	H bond Donors	Rotatable Bonds	Estimation of Drug likeness
a	368.385	3.8526	103.104	6	3	12	0.3902
b	368.385	3.8526	103.104	6	3	12	0.3902
c	368.385	3.8526	103.104	6	3	12	0.3902
d	368.385	3.8526	103.104	6	3	12	0.3902
e	368.385	3.8526	103.104	6	3	12	0.3902
f	368.385	3.8526	103.104	6	3	12	0.3902
g	368.385	3.8526	103.104	6	3	12	0.3902
h	368.385	3.8526	103.104	6	3	12	0.3902
i	368.385	3.8526	103.104	6	3	12	0.3902
j	368.385	3.3699	102.017	6	2	12	0.5481

3.5. Prediction of drug-like properties of Curcumin by using SwissADME

Table 2. Prediction of drug-like properties of Curcumin by using SwissADME.

MW: Molecular weight; LogP: Logarithm of partition coefficient of the compound between n-octanol and water; nHBA: Num. H-bond acceptors; nHBD: Num. H-bond donors; TPSA: Topological Polar Surface Area; nRotB: Num. rotatable bonds; SA: Synthetic accessibility.

Comp.	MW (Da)	Log P	nHBA	nHBD	TPSA (Å²)	nRotB	Drug-likeness		SA
							Lipinski	Verber	
	< 500	≤ 5	< 10	≤ 5	<140	<10	Yes/No		0 ≤SA ≤10
a	368.38	3.17	6	3	96.22	7	YES	YES	3.42
b	368.38	3.17	6	3	96.22	7	YES	YES	3.42
c	368.38	3.17	6	3	96.22	7	YES	YES	3.42
d	368.38	3.17	6	3	96.22	7	YES	YES	3.42
e	368.38	3.17	6	3	96.22	7	YES	YES	3.42
f	368.38	3.17	6	3	96.22	7	YES	YES	3.42
g	368.38	3.17	6	3	96.22	7	YES	YES	3.42
h	368.38	3.17	6	3	96.22	7	YES	YES	3.42
i	368.38	3.17	6	3	96.22	7	YES	YES	3.42
j	368.38	3.03	6	2	93.06	8	YES	YES	2.97

The drug-like property evaluation of curcumin rotamers including the diketone form was carried out by the SwissADME tool. Here all the structures were aligned with Lipinski's rule of five and the Verber's rule. This is a good indication of the favorable oral bioavailability and permeability characteristics (Mahal *et al.*, 2024). All the structures possessed the molecular weight of 368.38 Da which is below the threshold of 500 Da and avoid the structural bulkiness that typically hinders cellular uptake. While the LogP values with the range of (3.03-3.17) indicated the moderate lipophilicity suitable for membrane permeability without compromising aqueous solubility. The compounds possess sufficient hydrophobicity to partition into the lipid bilayer without triggering precipitation or poor dissolution in aqueous physiological fluids. Each structure possessed six Hydrogen bond acceptors and all the enolic structures have three Hydrogen Bond Donors. Meanwhile the diketone structure possessed only two Hydrogen Bond Donors. All these values supported the good pharmacokinetic balance with solubility and permeability. The topological surface area values (93.06 – 96.22 Å^2) remained below the threshold value of 140 Å^2 suggesting that these rotamers exhibit acceptable polar surface area for oral absorption and potential blood-brain barrier permeability. All the rotamer structures contributed fewer than ten rotatable bonds, indicating moderate molecular flexibility consistent with drug-like behavior. This structural trait allows the molecule to adapt to the active site pockets while avoiding the massive conformational entropic penalties that degrade the permeability of highly flexible chains. Since all rotamer structures maintained synthetic accessibility scores which matched with the given range, all the conformers are synthetically feasible with moderate ease. Collectively computed results supported the studied compounds possess favorable physicochemical and structural properties compatible with drug-like molecules. Obtained findings

underscored their importance in further docking, pharmacokinetic and biological activity analyses (Mahal *et al.*, 2024).

3.6 Prediction of ADMET properties of Curcumin by using pkCSM.

Table 3. Prediction of adsorption, distribution, excretion and toxicity of Curcumin isomers by using pkCSM

HIA: % Human intestinal absorption; P-Gp: P-glycoprotein substrate; BBB: Blood-Brain-Barrier permeability (log BB); CNS: Central nervous system permeability (log PS); TC: Total clearance (Log ml/min/kg).

Compound	Adsorption			Distribution		Excretion	Toxicity
	Solubility	HIA	P-Gp	BBB	CNS	TC	Ames
	>-4	>80%	No			0.5 - 1.5	
a	-4.01	82.19	Yes	-0.562	-2.99	-0.002	No
b	-4.191	71.721	Yes	-0.873	-2.887	0.075	No
c	-3.704	76.526	Yes	-1.047	-2.902	0.071	No
d	-4.004	71.568	Yes	-0.942	-2.887	0.075	No
e	-3.714	76.526	Yes	-1.047	-2.898	0.071	No
f	-3.862	76.679	Yes	-0.979	-2.898	0.071	No
g	-4.004	71.568	Yes	-0.942	-2.887	0.075	No
h	-4.191	71.721	Yes	-0.873	-2.887	0.075	No
i	-3.763	84.639	Yes	-0.997	-2.898	0.053	No
j	-3.885	81.727	Yes	-0.55	-2.963	-0.022	No

The pharmacokinetic and toxicity properties of the Curcumin rotamers were predicted by using pkCSM web server to identify the drug likeness and safety profile. The above table evaluated the parameters of absorption (solubility, human intestinal absorption and P-glycoprotein substrate behaviour), distribution (blood-brain barrier and central nervous system permeability), excretion (total clearance) and toxicity (Ames mutagenicity) (Mahal *et al.*, 2024).

The negative solubility values of all curcumin rotamers indicated that the considered structures show moderate to low aqueous solubility. Values around -4 or slightly below indicated low aqueous solubility, which corresponded to the low oral bioavailability. Human Intestinal Absorption values of the above drug candidates ranged between 71% to 84%. These values suggested moderate intestinal absorption. All compounds were predicted as P-glycoprotein substrates, implying that cellular efflux mechanisms may slightly limit intracellular accumulation but do not impede absorption efficiency.

Standard BBB permeability values (Log BB < 0.3) and CNS permeability values (LogPS <-2) below the specific threshold values confirm the unsuitability of penetrating the BBB and the central nervous system. Because the above values lie around -1, indicating poor BBB penetration. Further CNS permeability values are around -2.9 and indicated the very low CNS penetration. Due to this, these rotamers cannot be intended for brain targeting (Mahal *et al.*, 2024).

Total clearance values within the range of (-0.02 to 0.075 log ml^{-1} min^{-1} kg^{-1}) suggested that obtained values are extremely low and account for the slow excretion. Because of that, studied compounds persist in the body for an extended period of time which allows for reaching the intended therapeutic target.

All the Curcumin rotamers were non-mutagenic because the AMES toxicity results with "NO". This suggests that curcumin is safe and non-carcinogenic. The most important prediction of the pkCSM web tool is the toxicity analysis. All the computed structures are negative in the AMES mutagenicity assay, conforming to non-genotoxic and non-carcinogenic behaviour.

Overall, the pkCSM-predicted results indicate that curcumin rotamers possess good absorption, limited CNS distribution, acceptable clearance and low toxicity risk, fulfilling essential ADMET criteria for potential development as safe Histone deacetylase (HDAC) inhibitors.

3.7 Prediction of Metabolism of Curcumin by using pkCSM

Table 4. Prediction of Metabolism of Curcumin isomers by using pkCSM.

Compound	Metabolism				
	CYP1A2	CYP2C19	CYP2C9	CYP2D6	CYP3A4
a	Yes	Yes	Yes	No	Yes
b	No	Yes	Yes	No	Yes
c	Yes	Yes	Yes	No	Yes
d	No	Yes	Yes	No	Yes
e	Yes	Yes	Yes	No	Yes
f	Yes	Yes	Yes	No	Yes
g	No	Yes	Yes	No	Yes
h	No	Yes	Yes	No	No
i	Yes	Yes	Yes	No	Yes
j	Yes	Yes	Yes	No	Yes

The above table explains the potential interactions with key Cytochrome P450 isoenzymes by using the pkCSM tool. CYP1A2, CYP2C19, CYP2C9, CYP2D6, and CYP3A4, are the major enzymes which affect for the oxidative metabolism and detoxification of xenobiotics in aqueous environments (Mahal *et al.*, 2024). According to the obtained results Curcumin rotamers were potential substrates or inhibitors for at least three CYP isoforms, primarily CYP1A2, CYP2C9, and CYP3A4 which indicated its extensive phase 1 metabolism. Except a s-cis, s-cis, a structure all the other structures interacted with the CYP3A4 isoenzyme, which is involving in human drug metabolism. In the table optimal value was indicated as "No" due to concerns regarding toxicity or drug-drug interactions. Therefore, CYP2D6 was predicted to be negative for most rotamers, indicating a reduced risk of drug-drug interactions. According to the computed predictions studied, Curcumin compounds undergo extensive phase 1 and 2 metabolism, and there is a necessity for

formulation strategies or prodrug approaches to minimize metabolic liability (Mahal *et al.*, 2024).

4. Conclusions

A multi-faced computational approach was designed to identify a number of binding orientations within the Curcumin scaffold which causes inhibition of the HDAC active site. Geometry optimization and frequency analysis were implemented at the B3LYP 6-31+G(d) level in implicit solvent. The computed pKa values using thermodynamic cycle were highly negative (-15.1 to -16.9), indicating that the conjugate base of Curcumin is extremely stable in the solvent environment. The minimal variation among the rotamer values suggested that all rotamers possess similar electronic environments in DMSO media. Molecular docking studies revealed the crucial binding affinities of the rotamer structures to the HDAC enzyme, with all values ranging between -3.56 and -5.11 kcal mol^{-1} which indicate weak to moderate inhibitory activity towards the HDAC enzyme. The multiple QSAR results revealed that HOMO energy is the dominant factor affecting pIC_{50}, whereas the dipole moment and pKa have weaker and non-significant contributions. The strong model statistics (R^2 = 0.8047, F = 8.2389, P = 0.015) confirmed the selected combination of electronic descriptors was appropriate for predicting the inhibitory potential of Curcumin isomeric forms. All enolic rotamers and the diketone form exhibited drug-like behavior, with the diketone form demonstrating the best pharmacokinetic suitability, as evidenced by a drug-likeness value of 0.5481 compared to an enolic value of 0.3902. There was no difference in the drug-likeness value among the separate enolic rotamer structures, indicating that drug-likeness is not dependent on the spatial arrangement. In silico ADMET and toxicity evaluation of Curcumin rotamers using pkCSM and SwissADME demonstrated that all studied compounds possessed favorable pharmacokinetic and safety profiles. Overall, the present study provides preliminary computational insights into the interactions of Curcumin tautomers with HDAC8. Further structural optimization and experimental validation are required to confirm their inhibitory activity and assess their therapeutic relevance before any potential application as HDAC8 inhibitors can be considered.

Author Contributions

Conceptualization, G.P; methodology, G.P., O.A.D.B.P.; software, G. P., O.A.D.B.P.; validation, G.P.; formal analysis, G.P., O.A.D.B.P.; investigation, G.P.; resources, G.P., O.A.D.B.P.; data curation, G. P., O.A.D.B.P.; writing—original draft preparation, O.A.D.B.P.; writing—review and editing, G.P.; visualization, G.P., O.A.D.B.P.; supervision, G.P.; project administration, G.P. All authors have read and agreed to the published version of the manuscript.

Funding

This research received no external funding.

Acknowledgements

Department of Chemistry, Faculty of Science, Eastern University Sri Lanka is acknowledged.

Conflicts of Interest: The authors declare no conflict of interest.

References

Ali, S. T., Choudhary, A., Syed, M. K., and Zubair, A. (2021). A simple computational approach for pKa calculation of organosulfur compounds. *Journal of the Serbian Chemical Society*, 86(2), pp. 165–170. Available at: https://doi.org/10.2298/JSC200518042A.

Alisi, I.O., Uzairu, A. and Abechi, S.E. (2020). Molecular design of curcumin analogues with potent antioxidant properties and thermodynamic evaluation of their mechanism of free radical scavenge. *Bulletin of the National Research Centre*, 44(1). Available at: https://doi.org/10.1186/s42269-020-00391-z.

Bonab, M.I. *et al.* (2017). A computational study of the electronic structure and the chemical activity of curcumin and some novel curcuminoids by density functional theory. *Journal of the Iranian Chemical Society*, 14(2), pp. 357–364. Available at: https://doi.org/10.1007/s13738-016-0984-x.

Boulmokh, Y. *et al.* (2024). Enhanced antioxidant properties of novel curcumin derivatives: a comprehensive DFT computational study. *Structural Chemistry*, 35(3), pp. 825–839. Available at: https://doi.org/10.1007/s11224-023-02237-6.

Ferrari, I.V. (2024). Computation analysis of histone deacetylases with curcumin. *African Research Journal of Medical Sciences*, 1(2), pp. 58–61. Available at: https://doi.org/10.62587/afrjms.1.2.2024.58-61.

Kolev, T.M. *et al.* (2005). DFT and experimental studies of the structure and vibrational spectra of curcumin. *International Journal of Quantum Chemistry*, 102(6), pp. 1069–1079. Available at: https://doi.org/10.1002/qua.20469.

Li, Y. and Seto, E. (2016). HDACs and HDAC inhibitors in cancer development and therapy. *Cold Spring Harbor Perspectives in Medicine*, 6(10). Available at: https://doi.org/10.1101/cshperspect.a026831.

Mahal, A. *et al.* (2024). Molecular docking, drug-likeness and DFT study of some modified tetrahydrocurcumins as potential anticancer agents. *Saudi Pharmaceutical Journal*, 32(1). Available at: https://doi.org/10.1016/j.jsps.2023.101889.

Mckee, S.A. and Pogorelov, T. V (2019). Determining the pKa of Simple Molecules Using Gaussian 2009. (September), pp. 1–6. Available at: http://pogorelov.scs.illinois.edu/wp-content/uploads/2019/09/pKa_Estimations_Tutorial_web.pdf.

Naama, J.H. *et al.* (2013). Curcuminoids as antioxidants and theoretical study of stability of curcumin isomers in gaseous state. *Research on Chemical Intermediates*, 39(9), pp. 4047–4059. Available at: https://doi.org/10.1007/s11164-012-0921-2.

Nag, A. *et al.* (2018). Bent Keto Form of Curcumin, Preferential Stabilization of Enol by Piperine, and Isomers of Curcumin∩Cyclodextrin Complexes: Insights from Ion Mobility Mass Spectrometry. *Analytical Chemistry*, 90(15), pp. 8776–8784. Available at: https://doi.org/10.1021/acs.analchem.7b05231.

Nedyalkova, M.A. *et al.* (2019). Calculating the Partition Coefficients of Organic Solvents in Octanol/Water and Octanol/Air. *Journal of Chemical Information and Modeling*, 59(5), pp. 2257–2263. Available at: https://doi.org/10.1021/acs.jcim.9b00212.

Spassov, D.S. (2024). Binding Affinity Determination in Drug Design: Insights from Lock and Key, Induced Fit, Conformational Selection, and Inhibitor Trapping Models. *International Journal of Molecular Sciences*, 25(13). Available at: https://doi.org/10.3390/ijms25137124.

Truong, D.H. *et al.* (2025). HOO radical scavenging activity of curcumin I and III in physiological conditions: a theoretical investigation on the influence of acid-base equilibrium and tautomerism. *RSC Advances*, 15(8), pp. 5649–5664. Available at: https://doi.org/10.1039/d4ra07769e.